Turkish J. Eng. Env. Sci.
28 (2004) , 135 – 148.

An Interface Crack between a Graded Coating and a Homogeneous Substrate

Ali ŞAHİN
Niagara University, Department of Mathematics, 333 Dunleavy Hall, NY 14109, USA
e-mail: asahin@niagara.edu

Received 20.10.2003

Abstract

The basic interface crack problem in a nonhomogeneous coating with continuously varying elastic properties bonded to a homogeneous semi-infinite medium is examined. The problem is encountered in studying the fracture mechanics of functionally graded materials, which are mostly 2-phase particulate composites with continuously varying volume fractions. The objective of this study is to determine the effect of the material nonhomogeneity parameters and relative dimensions on the stress intensity factors (SIFs). With the application to fracture mechanics in mind, the main result given in this study is the SIFs and crack opening displacements (CODs) as a function of the nonhomogeneity and the length parameters for various loading conditions. Using integral transforms for the displacements in the plane strain crack problem, the mixed boundary conditions are analytically reduced to a system of singular integral equations that are solved numerically using certain approximate techniques.

Key words: FGMs, Mixed-mode loading, Singular integral equations, Stress intensity factors, Crack opening displacements.

Introduction

Various forms of composites and bonded materials have always been widely used in technological applications such as power generation, transportation, aerospace, and microelectronics. However, to meet the exacting demands of modern technologies, the use of homogeneous materials and standard composites is becoming more and more difficult so that a greater emphasis in current research is placed on material design; more specifically, on developing new materials or material systems tailored for specific applications. Increasing concerns with mechanical failure initiating at the interfacial regions require a better understanding of the interaction between flaws that may exist in these regions and applied loads and other environmental factors. The conventional approach to studying the thermomechanics of such materials is based on the assumption that the composite medium is piecewise homogeneous and the flaws may be represented by plane cuts or cracks. On the other hand, in most bonded materials the interfacial region appears to have a structure that is generally different than that of the adjacent materials. In many cases, such as in plasma spray coating, sputtering and ion plating and in some diffusion bonded materials, the thermomechanical properties of the region are graded in the sense that the interfacial region is a nonhomogeneous continuum of finite thickness with very steep property gradients.

In this study, it is assumed that the coating is a functionally graded material (FGM), which is a composite with a gradual compositional variation in the thickness direction. These continuous changes result in property gradients that can be adjusted by controlling the composition. In this sense, material property grading is just another means to get optimal performance from the material. Generally, the objective of the optimal design is to provide such

properties as stiffness, strength, toughness, ductility, hardness and wear, corrosion and temperature resistance wherever needed in the structural component. In this respect the concept of FGM provides material scientists and engineers with a highly versatile tool. One of the important potential applications of FGMs is, for example, their use as an interfacial zone in bonding dissimilar materials. By eliminating the abrupt change in thermomechanical properties along the interface through property grading, it is possible not only to reduce or eliminate the stress concentrations but also to increase the bonding strength quite considerably. For an in-depth review of processing, design and applications of FGMs and extensive references see Yamanouchi *et al.* (1990), Holt *et al.* (1993), Ilschner and Cherradi (1995), Shiota *et al.* (1997), Kaysser (1999), Trumble *et al.* (2001) and Pan *et al.* (2003).

Since the structure and thickness of the coating play an important role in determining the crack growth resistance parameters as well as the crack driving force, in this study we examine the underlying fracture mechanics problem in a layered medium. In layered materials there are generally 3 types of fracture problems, namely surface cracking and crack penetration, debonding and edge delamination. In this study only the problem of debonding is considered. It is assumed that the medium consists of a graded coating bonded to a homogeneous substrate and contains an interface crack (Figure 1). The related plane strain problem is solved under various loading conditions and for various values of the material nonhomogeneity parameter. For a brief review of the fracture problems in conventional composite materials see Erdogan (1972). The interface crack problem for a nonhomogeneous coating and a homogeneous substrate of finite thickness was studied by Chen and Erdogan (1996) under uniform loading conditions. The effect of thermal loading on a nonhomogeneous half plane was examined by Jin and Noda (1993) and the steady thermal stresses in an infinite plane containing an internal crack investigated by Noda and Jin (1993).

Formulation of the Problem

Consider the plane elasticity problem with an interface crack between nonhomogeneous coating and homogeneous semi-infinite substrate described in Figure 1. It is assumed that the equal and opposite tractions (normal and shear) acting on the crack surfaces are the only applied loads and $x = 0$ is a plane of symmetry. In the problem, the shear modulus of the coating is approximated by

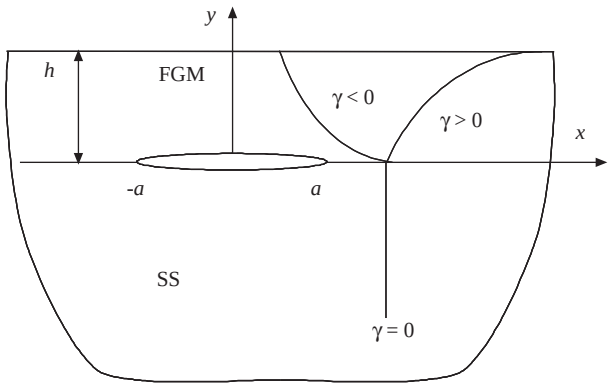

Figure 1. The geometry of a graded coating bonded to a homogeneous substrate.

$$\mu_1(y) = \mu_0 e^{\gamma y}, \qquad 0 < y \le h \tag{1}$$

where μ_0 is the shear modulus of the homogeneous substrate and the nonhomogeneity parameter γ may be positive or negative. Previous studies (Erdogan, 1972; Chen and Erdogan, 1996) indicate that the influence of Poisson's ratio ν on the stress intensity factors is not very significant. Therefore, ν may be assumed to be constant throughout the medium. Defining $\kappa = 3-4\nu$ for plane strain, stress-displacement relations may be written as

$$\sigma_{xx} = \frac{\mu_j}{\kappa - 1}\left((\kappa+1)\frac{\partial u_j}{\partial x} + (3-\kappa)\frac{\partial v_j}{\partial y}\right), \tag{2}$$

$$\sigma_{yy} = \frac{\mu_j}{\kappa - 1}\left((3-\kappa)\frac{\partial u_j}{\partial x} + (\kappa+1)\frac{\partial v_j}{\partial y}\right), \tag{3}$$

$$\sigma_{xy} = \mu_j\left(\frac{\partial u_j}{\partial y} + \frac{\partial v_j}{\partial x}\right), \qquad j = 0, 1. \tag{4}$$

Substituting from (1-4) into the equilibrium equations, it may be shown that

$$\begin{aligned}&(\kappa-1)\frac{\partial^2 u_j}{\partial y^2} + (\kappa+1)\frac{\partial^2 u_j}{\partial x^2} + 2\frac{\partial^2 v_j}{\partial x \partial y} + \\ &\gamma(\kappa-1)\frac{\partial u_j}{\partial y} + \gamma(\kappa-1)\frac{\partial v_j}{\partial x} = 0,\end{aligned} \tag{5}$$

$$(\kappa+1)\frac{\partial^2 v_j}{\partial y^2}+(\kappa-1)\frac{\partial^2 v_j}{\partial x^2}+2\frac{\partial^2 u_j}{\partial x\partial y}+ \gamma(3-\kappa)\frac{\partial u_j}{\partial x}+\gamma(\kappa+1)\frac{\partial v_j}{\partial y}=0 \tag{6}$$

where u_j and v_j, $(j=1,2)$, are the x and y components of the displacement, respectively, and $\gamma=0$ for $j=0$, $(y<0)$ and $\gamma\neq 0$ for $j=1$, $(0<y<h)$. By using Fourier transforms for displacements u_j and v_j and making use of the regularity conditions at $y=-\infty$, the solution of the system (5-6) may be expressed as

$$u_0(x,y)=\frac{1}{2\pi}\int_{-\infty}^{\infty}\sum_{k=1}^{2}b_k A_{0k}(\lambda)e^{|\lambda|y}e^{i\lambda x}d\lambda, \qquad y<0, \tag{7}$$

$$v_0(x,y)=\frac{1}{2\pi}\int_{-\infty}^{\infty}\sum_{k=1}^{2}d_k A_{0k}(\lambda)e^{|\lambda|y}e^{i\lambda x}d\lambda, \qquad y<0 \tag{8}$$

where

$$b_1=1, \quad b_2=y, \tag{9}$$

$$d_1=-i\frac{|\lambda|}{\lambda}, \qquad d_2=i\left(\frac{\kappa}{\lambda}-\frac{\lambda}{|\lambda|}y\right) \tag{10}$$

and $i=\sqrt{-1}$. Similarly, for the nonhomogeneous coating we obtain

$$u_1(x,y)=\frac{1}{2\pi}\int_{-\infty}^{\infty}\sum_{k=1}^{4}A_{1k}(\lambda)\,e^{m_k y}e^{i\lambda x}d\lambda, \quad 0<y\leq h, \tag{11}$$

$$v_1(x,y)=\frac{1}{2\pi}\int_{-\infty}^{\infty}\sum_{k=1}^{4}c_k A_{1k}(\lambda)\,e^{m_k y}e^{i\lambda x}d\lambda, \quad 0<y\leq h \tag{12}$$

where m_k and c_k, $(k=1,\ldots,4)$ are given by

$$m_1=\overline{m_3}=-\frac{\gamma}{2}+\frac{1}{2}R, \qquad m_2=\overline{m_4}=-\frac{\gamma}{2}-\frac{1}{2}R, \tag{13}$$

$$R=\sqrt{\gamma^2+4\lambda^2+4i\gamma\lambda\sqrt{\frac{3-\kappa}{\kappa+1}},} \tag{14}$$

$$c_k=-\frac{2i\lambda m_k+i\lambda\gamma(3-\kappa)}{(\kappa+1)m_k^2+\gamma(\kappa+1)m_k-\lambda^2(\kappa-1)}. \tag{15}$$

From the following boundary and continuity conditions

$$\sigma_{yy}(x,h)=0, \qquad -\infty<x<\infty, \tag{16}$$

$$\sigma_{xy}(x,h)=0, \qquad -\infty<x<\infty, \tag{17}$$

$$\sigma_{yy}(x,0^+)=\sigma_{yy}(x,0^-), \qquad -\infty<x<\infty, \tag{18}$$

$$\sigma_{xy}(x,0^+)=\sigma_{xy}(x,0^-), \qquad -\infty<x<\infty, \tag{19}$$

the unknown functions $A_{1k}(\lambda)$, $(k=1,\ldots,4)$, determined in terms of A_{01} and A_{02} as follows

$$A_{11}=\frac{w_1}{\Delta_2}A_{01}+\frac{w_2}{\Delta_2}A_{02}, \tag{20}$$

$$A_{12}=\frac{\overline{E_1}}{\Delta_2}A_{01}+\frac{\overline{E_2}}{\Delta_2}A_{02}, \tag{21}$$

$$A_{13}=\frac{\overline{w_1}}{\Delta_2}A_{01}+\frac{\overline{w_2}}{\Delta_2}A_{02}, \tag{22}$$

$$A_{14}=\frac{E_1}{\Delta_2}A_{01}+\frac{E_2}{\Delta_2}A_{02} \tag{23}$$

where w_k, E_k, $(k=1,2)$ and Δ_2 are defined in the Appendix. The remaining unknowns $A_{01}(\lambda)$ and $A_{02}(\lambda)$ may then be determined from the following mixed boundary conditions

$$v_1(x,0^+) = v_0(x,0^-), \qquad |a| < x, \tag{24}$$

$$u_1(x,0^+) = u_0(x,0^-), \qquad |a| < x, \tag{25}$$

$$\sigma_{1yy}(x,0^+) = \sigma_{0yy}(x,0^-) = -p_1(x), \quad -a < x < a, \tag{26}$$

$$\sigma_{1xy}(x,0^+) = \sigma_{0xy}(x,0^-) = -p_2(x), \quad -a < x < a \tag{27}$$

where the crack surface tractions p_1 and p_2 are known functions.

Derivation of the Integral Equations

To reduce the mixed boundary conditions (24-27) into a system of integral equations we first introduce the following new unknown functions (Erdogan *et al.*, 1973):

$$\phi_1(x) = \frac{\partial}{\partial x}\left(v_1(x,0^+) - v_0(x,0^-)\right), \tag{28}$$

$$\phi_2(x) = \frac{\partial}{\partial x}\left(u_1(x,0^+) - u_0(x,0^-)\right). \tag{29}$$

ϕ_1 and ϕ_2 must satisfy the following single-valuedness and symmetry conditions:

$$\int_{-a}^{a} \phi_j(s)ds = 0, \qquad \phi_j(x) = (-1)^j \phi_j(-x), \quad (j = 1,2). \tag{30}$$

In considering the boundary conditions (26) and (27), from (3) and (4) it can be shown that

$$\sigma_{0yy}(x,0^-) = \lim_{y\to 0^-} \frac{\mu_0}{2\pi} \int_{-\infty}^{\infty} \left[\left(\frac{\kappa+1}{|\lambda|} - 2y\right) A_{02} - 2A_{01}\right] e^{|\lambda|y} e^{i\lambda x} i\lambda d\lambda = -p_1(x), \tag{31}$$

$$\sigma_{0xy}(x,0^-) = \lim_{y\to 0^-} \frac{\mu_0}{2\pi} \int_{-\infty}^{\infty} \left[2A_{01} - \left(\frac{\kappa-1}{|\lambda|} - 2y\right) A_{02}\right] e^{|\lambda|y} e^{i\lambda x} \frac{d\lambda}{|\lambda|} = -p_2(x). \tag{32}$$

From the solution of the system in (5-6), the density functions can be written as

$$\phi_j(x) = \frac{1}{2\pi} \int_{-\infty}^{\infty} \sum_{k=1}^{2} s_{jk} A_{0k}(\lambda) e^{i\lambda x} d\lambda, \qquad (j = 1,2) \tag{33}$$

where s_{ij} are known algebraic functions of λ as defined in the Appendix. From (31)-(33)

$$\lim_{y\to o^-} \int_{-a}^{a} \phi_1(s)\, ds \int_0^{\infty} Z_{11}(\lambda)\, e^{\lambda y} \sin[\lambda(s-x)] + \lim_{y\to 0^-} \int_{-a}^{a} \phi_2(s)\, ds \int_0^{\infty} Z_{12}(\lambda)\, e^{\lambda y} \cos[\lambda(s-x)] d\lambda = -\tfrac{2\pi}{\mu_0} p_1(x), \tag{34}$$

$$\lim_{y\to 0^-} \int_{-a}^{a} \phi_1(s)\, ds \int_0^{\infty} Z_{21}(\lambda)\, e^{\lambda y} \cos[\lambda(s-x)] d\lambda + \lim_{y\to 0^-} \int_{-a}^{a} \phi_2(s)\, ds \int_0^{\infty} Z_{22}(\lambda)\, e^{\lambda y} \sin[\lambda(s-x)] d\lambda = -\tfrac{2\pi}{\mu_0} p_2(x). \tag{35}$$

To separate possible singular parts of $Z_{ij}(\lambda)$, $(i,j=1,2)$, in (34) and (35) the asymptotic behavior of the inner integrals must be examined. We observe that for $\lambda \to \infty$ the integrands of the inner integrals approach infinity. To eliminate these singularities at $\lambda \to \infty$, we may write the inner integrals in the following form:

$$\lim_{y\to o^-}\int_o^\infty \left(Z_{ij}(\lambda,y)-Z_{ij}^\infty(\lambda,y)\right)\sin\left[\lambda(s-x)\right]d\lambda+\lim_{y\to o^-}\int_0^\infty Z_{ij}^\infty(\lambda,y)\sin\left[\lambda(s-x)\right]d\lambda, \quad (i=j), \tag{36}$$

$$\lim_{y\to o^-}\int_0^\infty \left(Z_{ij}(\lambda,y)-Z_{ij}^\infty(\lambda,y)\right)\cos\left[\lambda(s-x)\right]d\lambda+\lim_{y\to 0^-}\int_0^\infty Z_{ij}^\infty(\lambda,y)\cos\left[\lambda(s-x)\right]d\lambda, \quad (i\neq j) \tag{37}$$

where $Z_{ij}^\infty(\lambda,y)$ are the asymptotic values of $Z_{ij}(\lambda,y)$ for large values of λ. Using the following identities

$$\lim_{y\to 0^-}\int_0^\infty e^{\lambda y}\sin\left[\lambda(s-x)\right]d\lambda=\frac{s-x}{y^2+(s-x)^2}, \tag{38}$$

$$\lim_{y\to 0^-}\int_0^\infty e^{\lambda y}\cos\left[\lambda(s-x)\right]d\lambda=\frac{y}{y^2+(s-x)^2}, \tag{39}$$

the system of integral equations (34-35) may be reduced to

$$\frac{1}{\pi}\int_{-a}^{a}\sum_{j=1}^{2}\left[\frac{\delta_{ij}}{s-x}+k_{ij}(x,s)\right]\phi_j(s)\,ds=-\frac{\kappa+1}{2\mu_0}p_i(x), \quad -a<x<a, \quad (i=1,2) \tag{40}$$

where the Fredholm kernels $k_{ij}(x,s)$ are square integrable in $-a\le(x,s)\le a$ (Erdogan *et al.*, 1973) and are given by

$$k_{ij}(x,s)=\int_o^\infty \left(Z_{ij}(\lambda,0)-Z_{ij}^\infty(\lambda,0)\right)\sin\left[\lambda(s-x)\right]d\lambda, \qquad (i=j),(i,j=1,2), \tag{41}$$

$$k_{ij}(x,s)=\int_o^\infty \left(Z_{ij}(\lambda,0)-Z_{ij}^\infty(\lambda,0)\right)\cos\left[\lambda(s-x)\right]d\lambda, \qquad (i\neq j),(i,j=1,2). \tag{42}$$

The functions $Z_{ij}(\lambda,y)$, $(i,j=1,2)$, are given in the Appendix. In (40), note that the singular term $\frac{1}{s-x}$ in the kernel is associated with the interface crack in a homogeneous medium and leads to the standard square-root singularity for the unknown functions $\phi_j(s)$. Next we note that by using the asymptotic expansions for $\lambda\to\infty$, the integrands in (41) and (42) may be expressed as

$$Z_{11}(\lambda,0)-Z_{11}^\infty(\lambda,0)=\frac{(\kappa+5)\gamma}{(\kappa+1)^2\lambda}+O\left(\frac{1}{\lambda^2}\right), \tag{43}$$

$$Z_{22}(\lambda,0)-Z_{22}^{\infty}(\lambda,0)=\frac{\gamma}{(\kappa+1)\lambda}+O\left(\frac{1}{\lambda^2}\right), \tag{44}$$

$$Z_{12}(\lambda,0)-Z_{12}^{\infty}(\lambda,0)=-\left(Z_{21}(\lambda,0)-Z_{21}^{\infty}(\lambda,0)\right)=\frac{\gamma}{(\kappa+1)\lambda}+O\left(\frac{1}{\lambda^2}\right). \tag{45}$$

Upon solving the integral equations (40) the modes I and II stress intensity factors at the crack tip $x=a$ may be evaluated from

$$k_1(a)=\lim_{x\to a}\sqrt{2(x-a)}\sigma_{yy}(x,0)=-\lim_{x\to a}\frac{2\mu_0}{\kappa+1}\sqrt{2(x-a)}\phi_1(x), \tag{46}$$

$$k_2(a)=\lim_{x\to a}\sqrt{2(x-a)}\sigma_{xy}(x,0)=-\lim_{x\to a}\frac{2\mu_0}{\kappa+1}\sqrt{2(x-a)}\phi_2(x). \tag{47}$$

Solution of Integral Equations

After the normalizations

$$s=at, \qquad x=ar, \qquad \phi_j(s)=\psi_j(t), \tag{48}$$

by defining

$$\psi_1(t)=\frac{1}{\sqrt{1-t^2}}\sum_{1}^{\infty}A_nT_{2n-1}(t), \tag{49}$$

$$\psi_2(t)=\frac{1}{\sqrt{1-t^2}}\sum_{1}^{\infty}B_nT_{2n}(t) \tag{50}$$

from (30) it may be shown that $A_0=0$, $B_0=0$ and Eq. (40) may be reduced to

$$\sum_{n=1}^{\infty}A_na_{in}(r_i)+\sum_{n=1}^{\infty}B_nb_{in}(r_i)=p_1(r_i), \tag{51}$$

$$\sum_{n=1}^{\infty}A_nc_{in}(r_i)+\sum_{n=1}^{\infty}B_nd_{in}(r_i)=p_2(r_i) \tag{52}$$

where a_{in}, b_{in}, c_{in} and d_{in} are known functions defined at each collocation point r_i by

$$a_{in}(r_i)=U_{2n-2}(r_i)+I_{11,n}(r_i)+\int_0^{\pi}\cos\left[(2n-1)\theta\right]X_{11}(\cos\theta,r_i)d\theta, \tag{53}$$

$$b_{in}(r_i) = I_{12,n}(r_i) + \int_0^{\pi} \cos[2n\theta] X_{12}(\cos\theta, r)\, d\theta, \tag{54}$$

$$c_{in}(r_i) = I_{21,n}(r_i) + \int_0^{\pi} \cos[(2n-1)\theta] X_{21}(\cos\theta, r)\, d\theta, \tag{55}$$

$$d_{in}(r_i) = U_{2n-1}(r_i) + I_{22,n}(r_i) + \int_0^{\pi} \cos[2n\theta] X_{22}(\cos\theta, r)\, d\theta. \tag{56}$$

The functions $I_{ij,n}(r)$ and $X_{ij}(\cos\theta, r)$ are given in the Appendix. By using the following properties of Chebyshev polynomials

$$\frac{1}{\pi}\int_{-1}^{1} \frac{T_k(t)}{(t-r)\sqrt{1}-t^2} dt = \begin{cases} 0, & k=0, \quad 1- < r < 1 \\ U_{k-1}(r), & k>0, \quad -1 < r < 1 \\ \frac{\left(\sqrt{r^2-1}-r\right)^k}{(-1)^{k+1}\sqrt{r^2-1}}, & k \geq 0, \quad |r| > 1 \end{cases} \tag{57}$$

$$\frac{1}{\pi}\int_{-1}^{1} \frac{T_k(t)}{\sqrt{1-t^2}} \log(|t-r|)\, dt = -\frac{T_k(r)}{k}, \qquad k \geq 1,\ |r| < 1, \tag{58}$$

$$\frac{1}{\pi}\int_{-1}^{1} \frac{T_k(t)}{\sqrt{1-t^2}} \frac{|t-r|}{t-r} dt = -2U_{k-1}(r)\sqrt{1-r^2}, \qquad k \geq 1,\ |r| < 1, \tag{59}$$

truncating the series in (51) and (52) at $n = N$ and by solving (51) and (52) for A_n and B_n, the stress intensity factors, the strain energy release rate and the crack opening displacements may be obtained as

$$k_1(a) = -\lim_{x\to a} \frac{2\mu_0}{\kappa+1}\sqrt{a}\sum_1^N A_n(x), \tag{60}$$

$$k_2(a) = -\lim_{x\to a} \frac{2\mu_0}{\kappa+1}\sqrt{a}\sum_1^N B_n(x), \tag{61}$$

$$G(a) = \frac{\pi(\kappa+1)}{8\mu_0}\left[(k_1(a))^2 + (k_2(a))^2\right], \tag{62}$$

$$V(x) = \frac{v_1(x,0^+) - v_0(x,0^-)}{v_0} = -\frac{\sqrt{1-(x/a)^2}}{P_1}\sum_{n=1}^{N} A_n \frac{U_{2n-2}(x/a)}{2n-1}, \tag{63}$$

$$U(x) = \frac{u_1(x,0^+) - u_0(x,0^-)}{u_0} = -\frac{\sqrt{1-(x/a)^2}}{P_2}\sum_{n=1}^{N} B_n \frac{U_{2n-1}(x/a)}{2n} \tag{64}$$

where P_1 and P_2 are the amplitudes of p_1 and p_2, respectively, and

$$v_0 = \frac{\kappa+1}{2\mu_0} aP_1, \qquad u_0 = \frac{\kappa+1}{2\mu_0} aP_2. \tag{65}$$

are constants.

Conclusion

The main results presented in this study are modes I and II stress intensity factors at the crack tips and the normalized crack opening displacements calculated for arbitrary crack surface tractions. The crack surface tractions $p_1(x)$ and $p_2(x)$ may be approximated by polynomials of the form

$$p(x) = p_0 + p_2\left(\frac{x}{a}\right)^2 + p_4\left(\frac{x}{a}\right)^4 + p_6\left(\frac{x}{a}\right)^6, \tag{66}$$

$$q(x) = q_1\left(\frac{x}{a}\right) + q_3\left(\frac{x}{a}\right)^3 + q_5\left(\frac{x}{a}\right)^5 + q^7\left(\frac{x}{a}\right)^7. \tag{67}$$

The dimensionless variables in the problem are γa and h/a. In Figures 2-14 the stress intensity factors and crack opening displacements are shown for 2 different loading conditions, namely $p_1(x) = -p_0$, $p_2(x) = 0$ and $p_1(x) = 0$, $p_2(x) = -q_1(x/a)$. The results are obtained by varying γa and h/a and for $\nu = 0.3$. In Tables 1-3 the effects of various crack surface tractions on the stress intensity factors are tabulated for different h/a and γa.

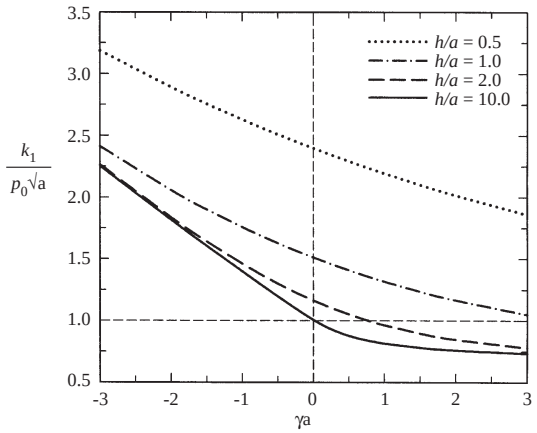

Figure 2. Mode I SIFs for various length parameters h/a under normal loading.

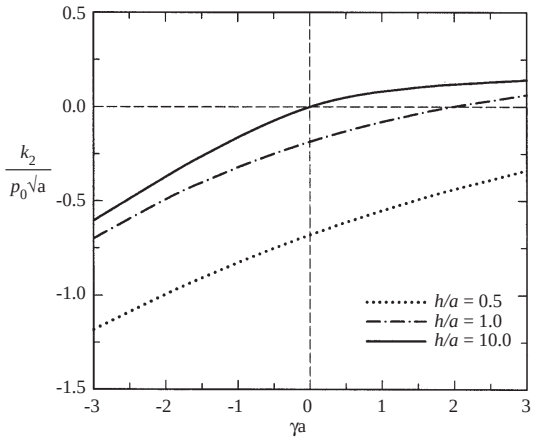

Figure 3. Mode II SIFs for various length parameters h/a under normal loading.

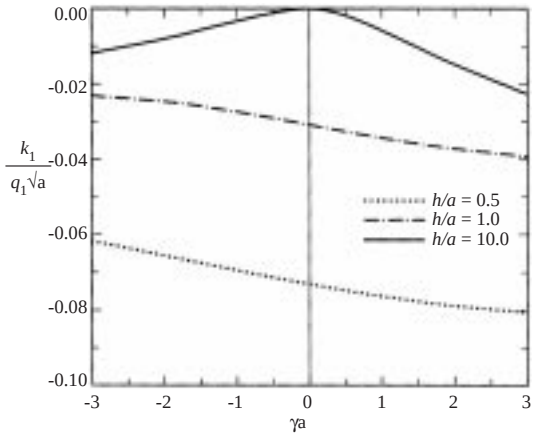

Figure 4. Mode I SIFs for various length parameters h/a under shear loading.

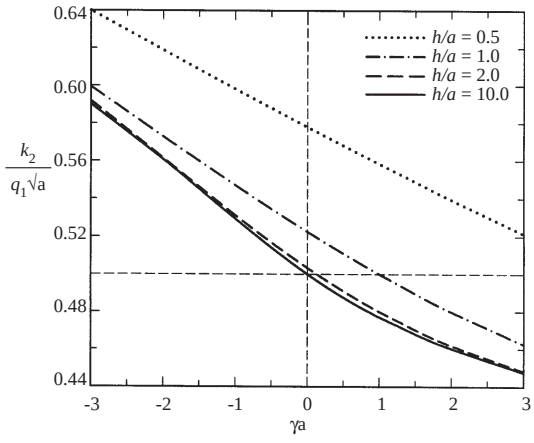

Figure 5. Mode II SIFs for various length parameters h/a under shear loading.

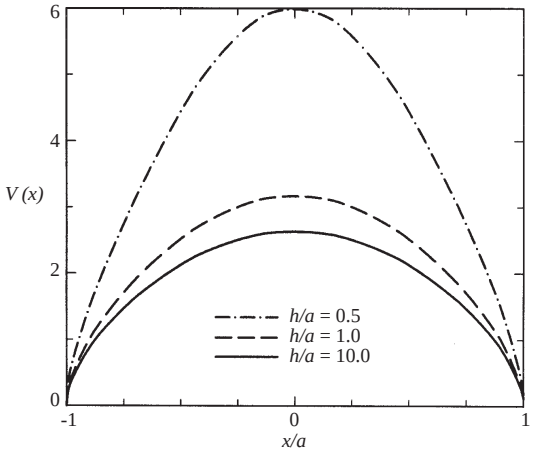

Figure 6. Normalized COD $V(x)$for $\gamma a = -2.0$, $\sigma_{yy}(x,0) = -p_0$ and $\sigma_{xy}(x,0) = 0$.

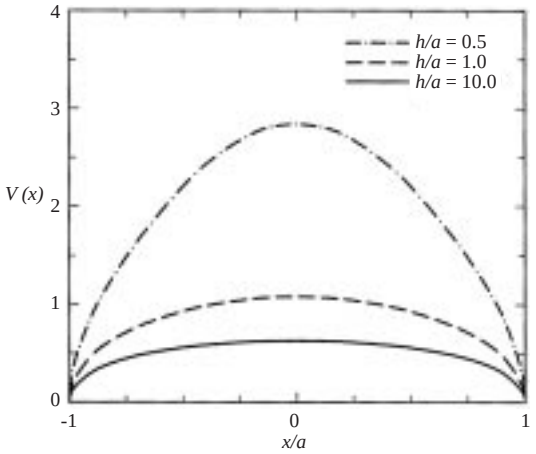

Figure 7. Normalized COD $V(x)$for $\gamma a = 2.0$, $\sigma_{yy}(x,0) = -p_0$ and $\sigma_{xy}(x,0) = 0$.

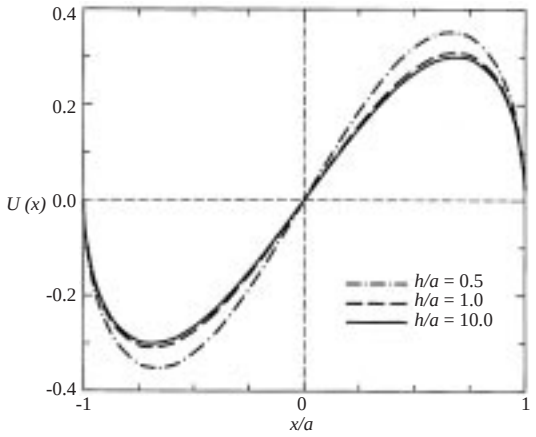

Figure 8. Normalized COD $U(x)$for $\gamma a = -2.0$, $\sigma_{yy}(x,0) = 0$ and $\sigma_{xy}(x,0) = -q_1\,(x/a)$.

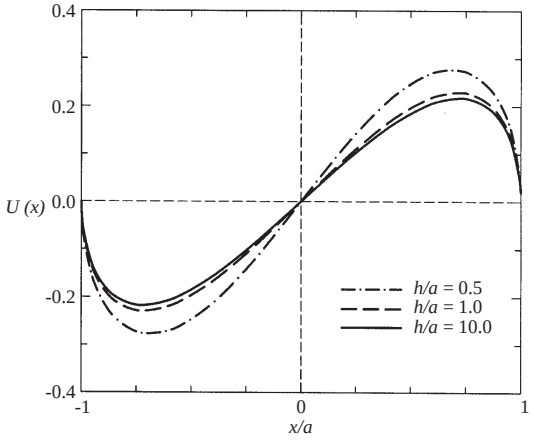

Figure 9. Normalized COD $U(x)$for $\gamma a = 2.0$, $\sigma_{yy}(x,0) = 0$ and $\sigma_{xy}(x,0) = -q_1\,(x/a)$.

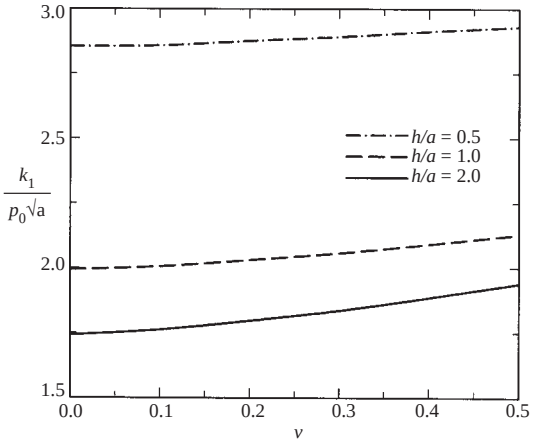

Figure 10. Mode I SIFs versus ν for various length parameters, $\gamma a = -2.0$.

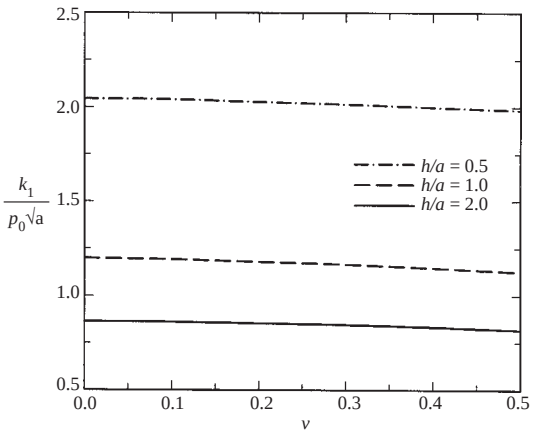

Figure 11. Mode I SIFs versus ν for various length parameters, $\gamma a = 2.0$.

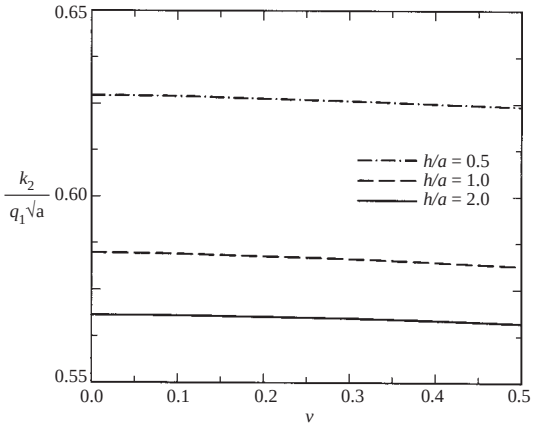

Figure 12. Mode II SIFs versus ν for various length parameters, $\gamma a = -2.0$.

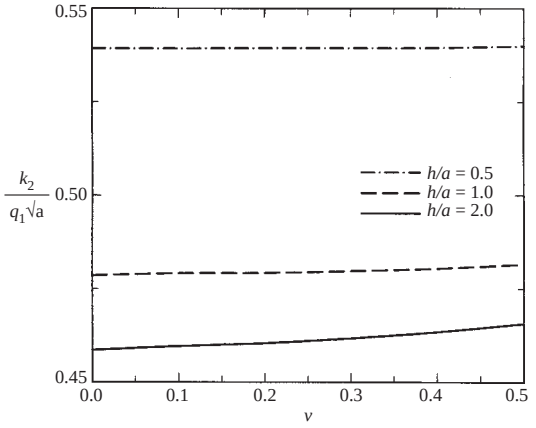

Figure 13. Mode II SIFs versus ν for various length parameters, $\gamma a = 2.0$.

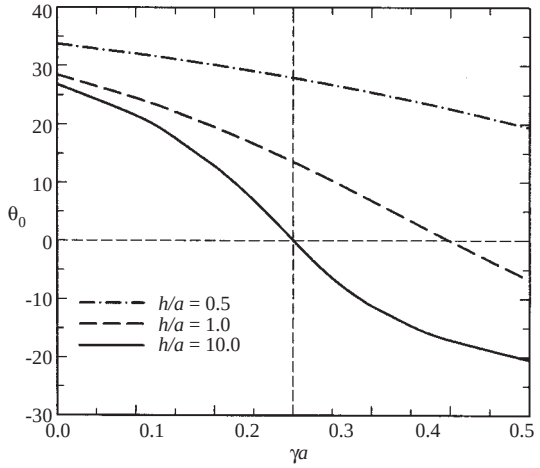

Figure 14. The crack extension angle θ_0 under normal loading, $\sigma_{yy}(x,0) = -p_0$ and $\sigma_{xy}(x,0) = 0$.

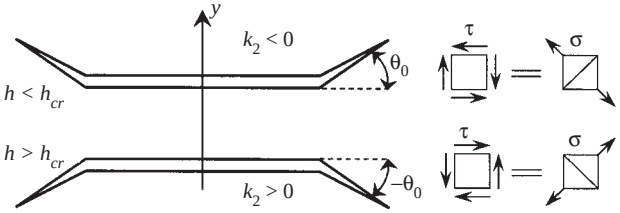

Figure 15. Possible crack extension direction.

When only normal tractions act on the crack surfaces, that is, for $\sigma_{yy}(x,0) = -p_0$ and $\sigma_{xy}(x,0) = 0$, it was observed that normalized stress intensity factor k_1 decreases for all values of h/a as the nonhomogeneity parameter γa increases (Fig. 2). Under the same loading, k_2 increases with increasing γa for all values of h/a (Fig. 3). On the other hand under shear loading, $\sigma_{yy}(x,0) = 0$ and $\sigma_{xy}(x,0) = -q_1(x/a)$, primary stress intensity factork_2 decreases for all values of h/a with increasing γa (Fig. 5). Also under shear loading k_1 decreases for small values of h/a with increasingγa. However, for large values of h/a, k_1 first increases for negative values and then decreases for positive values of γa (Fig. 4). From the same figures it can be observed that the primary stress intensity factors k_1 and k_2, under normal and shear loadings respectively, increase with decreasing thickness of the coating for constant values of γa. For the homogeneous half plane, that is, for $\gamma = 0$ it may be seen that the calculated stress intensity factors k_1 and k_2 should be equal to the results given in Erdogan et al. (1973). The effect of different loading conditions on stress intensity factors k_1 and k_2 for constant γa and h/a are presented in Tables 1-3.

Figures 6-9 show some sample results for the normalized crack opening displacements (COD) $V(x)$ and $U(x)$ defined in (63-64). From Figures 6-7 it may be seen that the crack opening displacement $V(x)$ decreases significantly with increasing γa for all values of h/a. Similarly, the crack opening displacement $U(x)$ decreases with increasing γa for all values of h/a but the effect of nonhomogeneity is not significant (Fig. 8-9). It may also be observed from the same figures that decreasing thickness of coating increases the crack opening displacements.

As mentioned previously, the problem is solved by assuming that the Poisson's ratio is constant. The assumption can only be justified if the fracture mechanics parameters of interest, in this case the stress intensity factors, prove to be relatively insensitive to variations in the Poisson's ratio. In the problem considered, it is indeed observed that the primary stress

Table 1. SIFs versus h/a under various loading conditions for constant nonhomogeneity parameter γa.

	$\gamma a = -2.0, \quad \nu = 0.3$					
h/a	$p_2\,(x/a)^2$		$p_4\,(x/a)^4$		$p_6\,(x/a)^6$	
	$\frac{k_1}{p_2\sqrt{a}}$	$\frac{k_2}{p_2\sqrt{a}}$	$\frac{k_1}{p_4\sqrt{a}}$	$\frac{k_2}{p_4\sqrt{a}}$	$\frac{k_1}{p_6\sqrt{a}}$	$\frac{k_2}{p_6\sqrt{a}}$
0.5	0.9557	–0.2096	0.5999	–0.0950	0.4526	–0.0557
1.0	0.7722	–0.1122	0.5150	–0.0534	0.4023	–0.0324
2.0	0.7242	–0.0895	0.4928	–0.0433	0.3891	–0.0265
10.0	0.7201	–0.0878	0.4909	–0.0426	0.3879	–0.0261
h/a	$q_3\,(x/a)^3$		$q_5\,(x/a)^5$		$q_7\,(x/a)^7$	
	$\frac{k_1}{q_3\sqrt{a}}$	$\frac{k_2}{q_3\sqrt{a}}$	$\frac{k_1}{q_5\sqrt{a}}$	$\frac{k_2}{q_5\sqrt{a}}$	$\frac{k_1}{q_7\sqrt{a}}$	$\frac{k_2}{q_7\sqrt{a}}$
0.5	–0.0335	0.4359	–0.0211	0.3514	–0.0149	0.3011
1.0	–0.0123	0.4138	–0.0077	0.3379	–0.0054	0.2919
2.0	–0.0049	0.4084	–0.0031	0.3347	–0.0022	0.2898
10.0	–0.0042	0.4081	–0.0027	0.3345	–0.0020	0.2896

Table 2. SIFs versus h/a under various loading conditions for constant nonhomogeneity parameter γa.

	$\gamma a = 0.001, \quad \nu = 0.3$					
h/a	$p_2\,(x/a)^2$		$p_4\,(x/a)^4$		$p_6\,(x/a)^6$	
	$\frac{k_1}{p_2\sqrt{a}}$	$\frac{k_2}{p_2\sqrt{a}}$	$\frac{k_1}{p_4\sqrt{a}}$	$\frac{k_2}{p_4\sqrt{a}}$	$\frac{k_1}{p_6\sqrt{a}}$	$\frac{k_2}{p_6\sqrt{a}}$
0.5	0.8234	–0.1376	0.5297	–0.0608	0.4065	–0.0350
1.0	0.6200	–0.0396	0.4332	–0.0183	0.3482	–0.0109
2.0	0.5390	–0.0083	0.3942	–0.0040	0.3244	–0.0025
10.0	0.5009	0.0002	0.3754	0.0001	0.3127	0.0001
h/a	$q_3\,(x/a)^3$		$q_5\,(x/a)^5$		$q_7\,(x/a)^7$	
	$\frac{k_1}{q_3\sqrt{a}}$	$\frac{k_2}{q_3\sqrt{a}}$	$\frac{k_1}{q_5\sqrt{a}}$	$\frac{k_2}{q_5\sqrt{a}}$	$\frac{k_1}{q_7\sqrt{a}}$	$\frac{k_2}{q_7\sqrt{a}}$
0.5	–0.0376	0.4125	–0.0238	0.3353	–0.0168	0.2891
1.0	–0.0152	0.3856	–0.0094	0.3189	–0.0066	0.2778
2.0	–0.0040	0.3765	–0.0025	0.3134	–0.0017	0.2741
10.0	–0.0001	0.3749	0.0000	0.3124	0.0000	0.2734

Table 3. SIFs versus h/a under various loading conditions for constant nonhomogeneity parameter γa.

	$\gamma a = 2.0, \quad \nu = 0.3$					
h/a	$p_2\,(x/a)^2$		$p_4\,(x/a)^4$		$p_6\,(x/a)^6$	
	$\frac{k_1}{p_2\sqrt{a}}$	$\frac{k_2}{p_2\sqrt{a}}$	$\frac{k_1}{p_4\sqrt{a}}$	$\frac{k_2}{p_4\sqrt{a}}$	$\frac{k_1}{p_6\sqrt{a}}$	$\frac{k_2}{p_6\sqrt{a}}$
0.5	0.7201	–0.0818	0.4741	–0.0339	0.3695	–0.0186
1.0	0.5190	–0.0067	0.3768	–0.0050	0.3099	–0.0037
2.0	0.4410	0.0305	0.3381	0.0161	0.2859	0.0104
10.0	0.4191	0.0328	0.3270	0.0172	0.2789	0.0111
h/a	$q_3\,(x/a)^3$		$q_5\,(x/a)^5$		$q_7\,(x/a)^7$	
	$\frac{k_1}{q_3\sqrt{a}}$	$\frac{k_2}{q_3\sqrt{a}}$	$\frac{k_1}{q_5\sqrt{a}}$	$\frac{k_2}{q_5\sqrt{a}}$	$\frac{k_1}{q_7\sqrt{a}}$	$\frac{k_2}{q_7\sqrt{a}}$
0.5	–0.0410	0.3907	–0.0261	0.3204	–0.0185	0.2779
1.0	–0.0189	0.3617	–0.0120	0.3026	–0.0085	0.2656
2.0	–0.0091	0.3530	–0.0059	0.2974	–0.0042	0.2620
10.0	–0.0079	0.3523	–0.0051	0.2969	–0.0037	0.2617

intensity factors k_1 and k_2 are relatively insensitive to variations in the Poisson's ratio (Fig. 10-13).

The possible crack extension angle θ_0 at the crack tip $x = a$ as measured from the x-axis is examined under normal loading p_0 for constant values of the coating thickness h/a. Defining h_{cr} as a critical coating thickness in which crack tip changes its direction either into the coating or into the substrate it may be shown the direction of crack extension in terms of the coating thickness. From Figure 14 it may be observed that θ_0 decreases with increasing nonhomogeneity parameter γa for all constant values of h/a. Note that in Figure 14 the crack extension angle θ_0 is always positive when the coating is less stiff than the substrate($\gamma a < 0$). On the other hand, for the stiff coatings ($\gamma a > 0$) the crack extension angle is positive for small values of the thickness of coating and then it becomes negative for large values of the coating thickness h/a. If the thickness of coating is sufficiently large, then θ_0 will always be negative for $\gamma a > 0$. This is qualitatively shown in Figure 15. From Figure 14, it may be seen that θ_0 becomes zero (crack extension along x-axis) for homogeneous infinite medium$\gamma a = 0$.

Appendix

$$\alpha_k = (\kappa + 1)\, m_k c_k + i\lambda\,(3 - \kappa)\,, \qquad \beta_k = m_k + i\lambda c_k. \tag{68}$$

$$\zeta_1 = \frac{-\overline{\alpha_1}\beta_2 - \alpha_2\overline{\beta_1}}{\Delta_1}, \qquad \zeta_2 = \frac{\alpha_2\beta_1 - \alpha_1\beta_2}{\Delta_1}. \tag{69}$$

$$\Delta_1 = \alpha_1\overline{\beta_1} + \alpha_1\beta_1 = \overline{\Delta_1}, \qquad \rho = \frac{1}{2}R. \tag{70}$$

$$G_1 = \alpha_1\zeta_1 e^{-\rho h} - \overline{\alpha_1}\zeta_2 e^{-(\rho+\overline{\rho})h/2} + \alpha_2, \qquad G_2 = \beta_1\zeta_1 e^{-\rho h} + \overline{\beta_1}\zeta_2 e^{-(\rho+\overline{\rho})h/2} + \beta_2. \tag{71}$$

$$\omega_1 = -2i\lambda\,(\kappa - 1)\,, \qquad \omega_2 = i\left(\kappa^2 - 1\right)\frac{\lambda}{|\lambda|}, \qquad \omega_3 = 2|\lambda|, \qquad \omega_4 = (\kappa - 1)\,. \tag{72}$$

$$E_1 = G_1\omega_3 - G_2\omega_1, \qquad E_2 = -G_1\omega_4 - G_2\omega_2. \tag{73}$$

$$\Delta_2 = G_1\overline{G_2} + \overline{G_1}G_2 = \overline{\Delta_2}. \tag{74}$$

$$w_1 = \left(\zeta_1\overline{E_1}e^{-\rho h} + \overline{\zeta_2}E_1 e^{-(\rho+\overline{\rho})h/2}\right), \qquad w_2 = \left(\zeta_1\overline{E_2}e^{-\rho h} + \overline{\zeta_2}E_2 e^{-(\rho+\overline{\rho})h/2}\right). \tag{75}$$

$$\Lambda_1(\lambda) = i\lambda\left(c_1 w_1 + c_2\overline{E_1} - \overline{c_1 w_1} - \overline{c_2}E_1 + i\Delta_2\frac{\lambda}{|\lambda|}\right), \tag{76}$$

$$\Lambda_2(\lambda) = i\lambda\left(c_1 w_2 + c_2\overline{E_2} - \overline{c_1 w_2} - \overline{c_2}E_2 - i\Delta_2\frac{\kappa}{\lambda}\right), \tag{77}$$

$$\Lambda_3(\lambda) = i\lambda\left(w_1 + \overline{E_1} + \overline{w_1} + E_1 - \Delta_2\right), \tag{78}$$

$$\Lambda_4(\lambda) = i\lambda\left(w_2 + \overline{E_2} + \overline{w_2} + E_2\right). \tag{79}$$

$$s_{11}(\lambda) = \frac{\Lambda_1}{\Delta_2}, \qquad s_{12}(\lambda) = \frac{\Lambda_2}{\Delta_2}, \qquad s_{21}(\lambda) = \frac{\Lambda_3}{\Delta_2}, \qquad s_{22}(\lambda) = \frac{\Lambda_4}{\Delta_2}. \tag{80}$$

$$\Delta_3 = \Lambda_1\Lambda_4 - \Lambda_2\Lambda_3. \tag{81}$$

$$z_{11}(\lambda, y) = i\lambda\Delta_2\left(-2\frac{\Lambda_4}{\Delta_3} - \left(\frac{\kappa+1}{|\lambda|} - 2y\right)\frac{\Lambda_3}{\Delta_3}\right), \tag{82}$$

$$z_{12}(\lambda, y) = i\lambda\Delta_2\left(2\frac{\Lambda_2}{\Delta_3} + \left(\frac{\kappa+1}{|\lambda|} - 2y\right)\frac{\Lambda_1}{\Delta_3}\right), \tag{83}$$

$$z_{21}(\lambda, y) = \Delta_2\left(2|\lambda|\frac{\Lambda_4}{\Delta_3} + (\kappa - 1 - 2|\lambda|y)\frac{\Lambda_3}{\Delta_3}\right), \tag{84}$$

$$z_{22}(\lambda, y) = \Delta_2\left(-2|\lambda|\frac{\Lambda_2}{\Delta_3} - (\kappa - 1 - 2|\lambda|y)\frac{\Lambda_1}{\Delta_3}\right). \tag{85}$$

$$As\, y \to 0^-, \quad Z_{11}(\lambda) = i\left(z_{11}(-\lambda) - z_{11}(\lambda)\right), \quad Z_{12}(\lambda) = \left(z_{12}(\lambda) + z_{12}(-\lambda)\right), \tag{86}$$

$$Z_{21}(\lambda) = \left(z_{21}(\lambda) + z_{21}(-\lambda)\right), \quad Z_{22}(\lambda) = i\left(z_{22}(-\lambda) - z_{22}(\lambda)\right). \tag{87}$$

$$I_{11,n}(r) = \frac{\alpha(\kappa+5)}{4(\kappa+1)}\left(\frac{\sin\left[(2n-1)\arccos(r)\right]}{2n-1}\right), \tag{88}$$

$$I_{22,n}(r) = \frac{\alpha}{8}\left(2\frac{\sin\left[2n\,\arccos(r)\right]}{2n}\right), \tag{89}$$

$$I_{12,n}(r) = -\frac{\alpha}{4}\left(-\frac{T_{2n}(r)}{2n}\right), \tag{90}$$

$$I_{21,n}(r) = \frac{\alpha}{4}\left(-\frac{T_{2n-1}(r)}{2n-1}\right), \qquad n = 1, 2, 3, ... \tag{91}$$

$$X_{11}(t,r) = \frac{\kappa+1}{4\pi} H_{11}(t,r) - \frac{\alpha(\kappa+5)}{8(\kappa+1)} \frac{|t-r|}{(t-r)}, \tag{92}$$

$$X_{12}(t,r) = \frac{\kappa+1}{4\pi} H_{12}(t,r) + \frac{\alpha}{4\pi} \log(|t-r|), \tag{93}$$

$$X_{21}(t,r) = \frac{\kappa+1}{4\pi} H_{21}(t,r) - \frac{\alpha}{4\pi} \log(|t-r|), \tag{94}$$

$$X_{22}(t,r) = \frac{\kappa+1}{4\pi} H_{22}(t,r) - \frac{\alpha}{8} \frac{|t-r|}{(t-r)}. \tag{95}$$

Acknowledgment

This study was supported by the Research Council of Niagara University under the Grant number RSG0423.

References

Chen, Y.F. and Erdogan, F., "Interface Crack Problem for a Nonhomogeneous Coating Bonded to a Homogeneous Substrate", Journal of the Mechanics and Physics of Solids, 44, 771-787, 1996.

Erdogan, F., "Fracture Problems in Composite Materials", Journal of Engineering Fracture Mechanics, 4, 811-840, 1972.

Erdogan, F., Gupta, G.D. and Cook, T.S., Numerical Solution of Singular Integral Equations. In Method of Analysis and Solution of Crack Problems, Sih, G.C. (ed.), Noordhoff Int. Publ.: Leyden, 1973.

Holt, J.B., Koizumi, M., Hirai, T. and Munir, Z.A. (eds.), FGM-92, Proceedings of 2nd International Symposium on Functionally Gradient Materials. The American Ceramic Society, Westerville, OH, 1993.

Ilshner, B. and Cherradi, N. (eds.), FGM-94, Proceedings of 3rd International Symposium on Structural and Functional Gradient Materials. Presses Polytechniques et Universitaires Romandes, Lausanne, Switzerland, 1995.

Jin, Z-H. and Noda, N., "An Internal Crack Parallel to the Boundary of a Nonhomogeneous Half Plane Under Thermal Loading", International Journal of Engineering Science, 31, 793-806, 1993.

Kaysser, W.A. (ed.), Material Science Forum Functionally Graded Materials, Vol. 308-311, Trans Tech Publications. Enfield, New Hampshire, 1999.

Noda, N. and Jin, Z-H., "Steady Thermal Stresses in an Infinite Nonhomogeneous Elastic Solid Containing a Crack", Journal of Thermal Stresses, 16, 181-196, 1993.

Pan, W. Gong, J. Zhong, L. and Chen, L. (eds.), Functionally Graded Materials VII. Trans Tech Publications L, Switzerland, 2003.

Shiota, I. and Miyamoto, Y. (eds.), FGM-96, Proceedings of 4th International Symposium on Functionally Gradient Materials, Elsevier Science, Amsterdam, The Netherlands, 1997.

Trumble, K. Bowman, K. Reimanis, I. and Sampath, S. (eds.), Functionally Graded Materials 2000, Ceramic Transactions 114, The American Ceramics Society, Westerville, Ohio, 2001.

Yamanouchi, M., Koizumi, M., Hirai, T. and Shiota, I. (eds.), FGM-90, Proceedings of 1st International Symposium on Functionally Gradient Materials, FGM Forum, Tokyo, Japan, 1990.